

# Iranian Journal of Electrical and Electronic Engineering

Journal Homepage: ijeee.iust.ac.ir



# Improved Multi-Conductor Transmission Line Modeling of Transformer to Study Frequency Response

Ali Esmaeilvandi\*, Mohammad Hamed Samimi\*(C.A.) and Amir Abbas Shayegani Akmal\*

Abstract: This paper introduces an improved multi-conductor transmission line (MTL) model for transformers' high-frequency transient and frequency response analysis, overcoming limitations in traditional models that fail to capture complex electromagnetic interactions during high-frequency events, such as lightning strikes and switching operations. The model accurately reflects real-world transformer behaviors under transient conditions by integrating particle swarm optimization (PSO) for efficient parameter estimation and incorporating frequency-dependent losses. The combined use of PSCAD and Python minimizes computational overhead, enabling high-fidelity simulations closely aligned with experimental transformer data. Validation against real transformer measurements demonstrates the model's reliability in capturing high-frequency responses, essential for transformer diagnostics. This novel approach offers a practical tool for studying transformer frequency response analysis, which is an important tool in transformer diagnosis.

**Keywords:** Frequency-Dependent Losses, High-Frequency Modeling, MTL Model, Particle Swarm Optimization, Transformer Diagnostics.

#### 1 Introduction

P OWER transformers are crucial components in modern electrical power systems, facilitating efficient energy transmission and voltage regulation across extensive, interconnected networks. With the increasing penetration of renewable energy sources, the evolution of smart grids, and the growing reliance on power electronics, transformers are being subjected to more frequent and intense transient events. These high-frequency disturbances—arising from lightning strikes, switching operations, and faults—pose significant risks to transformer insulation integrity, winding structures, and overall operational reliability. Failure to accurately model and analyze these transient events can lead to severe consequences, including unexpected outages, costly maintenance, and compromised grid stability [1-3].

Iranian Journal of Electrical & Electronic Engineering, 2026.

Paper first received 15 Mar. 2025 and accepted 29 Aug. 2025.

\*The authors are with School of Electrical and Computer Engineering, College of Engineering, University of Tehran, Iran.

E-mails: ali.esmaeilvandi@ut.ac.ir., m.h.samimi@ut.ac.ir, shayegani@ut.ac.ir.

Corresponding Author: Mohammad Hamed Samimi.

Traditional transformer modeling approaches rely primarily on lumped-parameter circuit-based models, which are effective at low frequencies but struggle to capture the complex electromagnetic interactions that occur at higher frequencies. These models, while useful for steady-state and low-frequency transient studies, often fail to account for distributed parameters such as inductance, capacitance, and resistance transformer windings. As a result, they are inadequate for high-frequency transient analysis, leading to inaccurate predictions of voltage distributions, resonant frequencies, and insulation stress conditions. The limitations of these models necessitate adopting more sophisticated approaches capable of accurately capturing high-frequency phenomena [4-6].

To overcome these deficiencies, multi-conductor transmission line (MTL) models have emerged as a more accurate alternative, representing transformer windings as coupled transmission lines. MTL models provide a distributed representation of electromagnetic wave propagation along the windings, making them particularly useful for high-frequency transient analysis and frequency response assessment. Studies have demonstrated the effectiveness of MTL models in capturing transformer resonance characteristics and

identifying winding deformations [7-10]. However, conventional MTL models still face challenges in accurately incorporating frequency-dependent effects such as insulation losses, conductor skin effects, and dielectric dispersion, which play a significant role in high-frequency response behavior [2, 11-14].

Several approaches have been proposed to refine transformer modeling techniques. Researchers have investigated fractional-order modeling methods, which provide more flexibility in simulating frequency-dependent losses and non-ideal dielectric behaviors [15, 16]. Additionally, hybrid methods that integrate lumped circuit elements with MTL frameworks have shown promise in balancing computational efficiency with accuracy, particularly for transient analysis applications [17-19]. Finite element analysis (FEA) has also been used to refine MTL models by accounting for spatial variations in electrical properties. However, these techniques typically require significant computational resources and detailed transformer design data, which may not always be accessible [20-22].

Another critical aspect of high-frequency transformer modeling is parameter estimation. Many existing models require detailed transformer design data, including geometrical dimensions, material properties, and insulation characteristics, which are often unavailable due to manufacturer confidentiality. This lack of data leads to difficulties in constructing accurate models, limiting their applicability in practical transformer diagnostics. To address these challenges, data-driven approaches using artificial intelligence and optimization techniques such as genetic algorithms (GA) and particle swarm optimization (PSO) have been introduced to estimate unknown parameters with high accuracy while reducing reliance on proprietary data [23, 24].

Given the increasing need for reliable high-frequency transformer models, it is essential to develop a modeling approach that balances accuracy with computational efficiency. This study introduces an improved MTL model that addresses the limitations of conventional approaches by incorporating advanced parameter estimation techniques, frequency-dependent loss modeling, and an efficient computational framework.

The key innovations of this study include:

Efficient Parameter Estimation Using PSO: PSO is employed to optimize critical transformer parameters, reducing dependency on proprietary design data while ensuring accurate alignment between simulated and real transformer behavior.

Incorporation of Frequency-Dependent Loss Parameters: The model integrates conductive and dielectric loss mechanisms, providing a more accurate representation of high-frequency transient conditions and improving simulation fidelity across a broad frequency range.

Integration of PSCAD and Python for Computational Efficiency: By leveraging PSCAD's electromagnetic transient simulation capabilities and Python's optimization tools, the study minimizes computational overhead while maintaining high-resolution modeling accuracy, making the approach feasible for real-time diagnostic applications.

The proposed model is validated using experimental data from real transformer measurements, demonstrating its ability to accurately capture high-frequency responses. By bridging the gap between computational efficiency and modeling accuracy, this work offers a practical solution for predictive maintenance and transformer fault diagnosis. The advancements introduced in this study contribute to the development of robust transformer models that support the reliability and efficiency of modern power systems, particularly as high-frequency transient phenomena become more prevalent due to the rapid evolution of energy infrastructure.

#### 2 Methodology

This study develops and validates advanced MTL models for analyzing high-frequency transient and frequency responses in transformers. The methodology involves (1) constructing improved MTL models that incorporate both frequency-independent and frequency-dependent loss parameters, (2) optimizing model parameters through PSO to ensure alignment with real transformer behaviors, (3) integrating PSCAD and Python for streamlined and efficient simulations, and (4) validating the models using experimental data to confirm their accuracy and reliability.

# 2.1 Models

#### **Basic MTL model:**

The basic MTL model captures high-frequency interactions within transformer windings by treating each winding segment as an individual transmission line. This approach allows for a distributed representation of inductive, capacitive, resistive, and conductive properties along the windings, making it effective for simulating high-frequency transient behaviors.

The model assumes each winding segment is a transmission line that interacts with other winding segments. This interaction occurs through common electric and magnetic fields, represented as capacitances and mutual inductances in the equivalent circuit theory. Thus, the model relies on impedance [Z] and admittance [Y] matrices to represent relationships among the winding parameters, providing the basis for calculating current and voltage along each conductor. The

representation of the basic MTL model of a winding is depicted in Fig. 1. Each winding segment is considered a transmission line (shown as a solid line), and these segments are connected as series elements (shown as a dotted line). For each segment, sending and receiving voltage and current are defined, as described in the figure. The mathematical equations based on them are defined in matrix form.

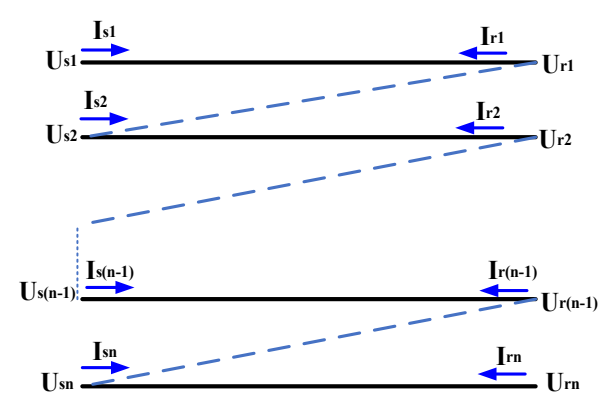


Fig 1. The MTL model for a transformer winding.

The governing differential equations for voltage and current are as follows [9]:

$$\frac{dU_i(x)}{dx} = -Z_{ii} \cdot I_i(x) - \sum_{i \neq i} Z_{ji} \cdot I_j(x)$$
 (1)

$$\frac{dI_{i}(x)}{dx} = -Y_{ii}.U_{i}(x) - \sum_{i \neq i} Y_{ji}.U_{j}(x)$$
 (2)

where  $U_i(x)$  is the voltage at position x along the i-th conductor,  $I_i(x)$  is the current at position x along the i-th conductor,  $Z_{ii}$  is the self-impedance of the i-th segment,  $Z_{ij}$  is the mutual impedance between segments i and j,  $Y_{ii}$  is the self-admittance of the i-th segment, and  $Y_{ij}$  is the Mutual admittance between segments i and j.

These equations can be represented in matrix form as [9]:

$$\frac{dU(x)}{dx} = -Z.I(x) \tag{3}$$

$$\frac{dI(x)}{dx} = -Y.U(x) \tag{4}$$

Where  $U(x) = [U_1(x), U_2(x), ..., U_m(x)]^T$  is the voltage vector,  $I(x) = [I_1(x), I_2(x), ..., I_m(x)]^T$  is the current vector, and Z and Y are the impedance and admittance matrices, respectively.

While effective under uniform propagation conditions, the basic MTL model has limitations in representing complex high-frequency behaviors, such as non-transverse electromagnetic modes, which restricts its application in scenarios requiring detailed frequency-dependent loss modeling.

#### **Improved MTL Model 1:**

To address the limitations of the basic MTL model, an improved version is introduced here, incorporating frequency-independent loss parameters to account for baseline conductive and insulation losses that remain constant across frequencies. These parameters are considered by adding a fixed resistive component, which improves the simulation of high-frequency transients without significantly increasing computational complexity. These resistors are shown in the model in Fig. 2. The series resistors between segments can model the losses in the conductors, while the resistors between segments and the ground represent the dielectric loss in the insulation system. These fixed resistive elements contribute to model stability and prevent unrealistic oscillations, enabling smoother transient behavior and enhancing the accuracy of high-frequency simulations.

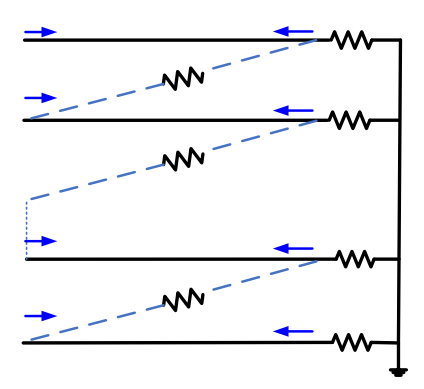


Fig 2.The MTL model of transformer winding with frequencyindependent losses.

In this improved model, frequency-independent losses are incorporated directly within the impedance matrix [Z], represented as:

$$Z = R + j\omega L \tag{5}$$

where R captures fixed resistive losses due to conductor and dielectric losses, and L is the inductance associated with each segment. The differential equations for this improved model are then modified as follows:

$$\frac{dU_i(x)}{dx} = -(Z_{ii} + R).I_i(x) - \sum_{j \neq i} Z_{ji}.I_j(x)$$
 (6)

$$\frac{dI_{i}(x)}{dx} = -Y_{ii}.U_{i}(x) - \sum_{j \neq i} Y_{ji}.U_{j}(x)$$
 (7)

In matrix form, these modified equations are:

$$\frac{dU(x)}{dx} = -(Z+R).I(x) \tag{8}$$

$$\frac{dI(x)}{dx} = -Y.U(x) \tag{9}$$

Frequency-independent losses are primarily associated with the inherent DC resistance of the transformer

conductors and minor leakage currents across the insulation material between windings and the ground. Each section of the transformer winding exhibits a resistive loss due to the DC resistance of the conductor material. This resistance changes with frequency but is assumed to remain constant across frequencies in this model. This resistance contributes to energy dissipation in the form of heat. In the improved MTL model, this is represented as a fixed resistive component in the impedance matrix [Z], ensuring that each transmission line section accurately reflects the real-world resistive losses in transformer windings. Furthermore, a fixed insulation resistance is included to represent leakage currents across insulation layers between windings or between windings and the ground. These leakage losses also depend on the frequency but are assumed to remain consistent across the frequency spectrum for simplicity. Incorporating them as frequency-independent parameters provides a stable foundation for the model's transient response. By treating these losses as constant, the model maintains computational efficiency without compromising reliability in high-frequency simulations.

Incorporating these series and ground-connected resistances directly within the impedance matrix [Z]enhances model stability and reduces computational load. Fixed resistive components prevent unrealistic oscillations and resonance in the high-frequency response, which can occur if only frequency-dependent parameters are used. These resistive elements provide a natural damping effect, resulting in smoother transient behavior and improving the fidelity of high-frequency simulations. Treating these losses as constants minimizes the need for repetitive recalculations based on frequency, reducing computational demand. This simplification is particularly advantageous in real-time applications, where computational efficiency is critical for rapid diagnostics and analysis.

While the inclusion of these resistive losses provides a robust baseline for high-frequency analysis, this approach has both strengths and limitations. The fixed resistive elements contribute to model stability and computational simplicity, making the model well-suited for real-time transformer diagnostics and condition monitoring. This stability also supports reliable results during high-frequency transient events. On the other hand, frequency-independent parameters do not capture the varying nature of losses that occur due to phenomena like dielectric losses and skin effects at very high frequencies. To address this, frequency-dependent parameters need to be modeled separately to account for these dynamic loss components.

# **Improved MTL Model 2:**

This enhanced MTL model uses frequency-dependent parameters for applications needing higher accuracy, capturing dielectric and conductor losses that change with frequency. By adjusting dynamically with frequency, the model offers a realistic view of insulation behavior under high-frequency transient conditions, which is crucial for effective transformer diagnostics and maintenance.

The dielectric loss is usually represented as the dielectric dissipation factor or  $tan\delta$ . The dielectric loss angle  $\delta$  quantifies the extent of energy dissipation within the insulation material and varies with frequency. For oil-impregnated paper insulation, the dielectric loss angle can be expressed as [2]:

$$tan(\delta) = 1.082 \times 10^{-8} \omega + 0.005$$
 (10) where  $\omega$  is the angular frequency. As frequency increases, insulation losses rise, contributing to greater dielectric heating and energy dissipation. Without

dielectric heating and energy dissipation. Without modeling these variations, high-frequency transformer simulations may underestimate losses, leading to inaccurate transient response predictions.

equivalent dielectric resistance  $R_{dielectric}$ representing the resistive losses within the insulation, is inversely related to the dielectric loss angle and frequency. It is calculated by [2]:

$$R_{dielectric} = \frac{1}{\omega C_h tan\delta}$$
 (11)

where  $C_h$  is the capacitance associated with each section of the winding. This relationship allows the improved model to dynamically adjust for varying insulation losses that increase with frequency, enhancing its accuracy in transient simulations. In this model,  $R_{dielectric}$ lies parallel with the winding capacitance in each section as depicted in Fig. 3. It is noteworthy that the dependency of the series resistor on frequency is neglected in this model too, since the dependency of the conductor losses on frequency does not play an important role in the high-frequency response of the winding.

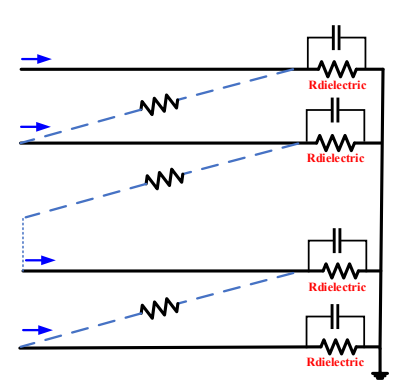


Fig 3. The modified MTL model for transformer windings with frequency-dependent loss.

By incorporating this resistance, the impedance and admittance matrices are then updated as:

$$Z = R + R_{dielectric}(\omega) + j\omega L \tag{12}$$

$$Y = G + i\omega C \tag{13}$$

where R represents the conductor resistance matrix, capturing DC resistive losses within the transformer,  $R_{dielectric}(\omega)$  is the matrix of frequency-dependent dielectric resistances, L denotes the inductance matrix for each segment of the winding, G is the conductance matrix accounting for shunt insulation properties, and C is the capacitance matrix associated with each section of the transformer winding.

The governing differential equations for this improved model are:

$$\frac{dU_{i}(x)}{dx} = -(Z_{ii} + R_{dielectric}(\omega)) \cdot I_{i}(x) 
- \sum_{j \neq i} Z_{ji} \cdot I_{j}(x)$$

$$\frac{dI_{i}(x)}{dx} = -(G_{ii} + \frac{1}{R_{dielectric}(\omega)}) \cdot U_{i}(x)$$

$$\sum_{j \neq i} V_{i} U_{i}(x)$$
(15)

$$\frac{dI_{i}(x)}{dx} = -(G_{ii} + \frac{1}{R_{dielectric}(\omega)}) \cdot U_{i}(x) - \sum_{j \neq i} Y_{ji} \cdot U_{j}(x)$$

$$(15)$$

In matrix form, these equations become:

$$\frac{dU(x)}{dx} = -(Z + R_{dielectric}(\omega)).I(x)$$
 (16)

$$\frac{dI(x)}{dx} = -(G + \frac{1}{R_{dilectric}(\omega)})U(x)$$
 (17)

By incorporating frequency-dependent losses, this improved model offers greater accuracy in representing the real-world behavior of high-frequency transformers, making it a robust tool for transient response analysis, fault diagnostics, and predictive maintenance.

# 2.2 Parameter Estimation Using Particle Swarm **Optimization (PSO)**

The parameter estimation process is critical for aligning the improved MTL model with real transformer behaviors. To achieve this, PSO is employed, an algorithm well-suited for optimizing complex models with multiple parameters. PSO is particularly effective here due to its fast convergence and capability to search high-dimensional parameter spaces efficiently.

PSCAD has a transmission line model for simulating overhead transmission lines. In order to use the complete transmission line formulation of the software for the transformer modeling purpose, the same transmission line module is employed. For this purpose, a transmission line with seven conductors is defined in the software, where these conductors are located in the air near each other as shown in Fig. 4. In an MTL model, the winding is subdivided into multiple sections, with section represented by a corresponding transmission line model. In this study, the winding is divided into seven sections, and each conductor in the simulation model represents the transmission line model for these sections. The conductors are placed in close proximity to one another, resulting in both electrostatic (capacitive) and magnetic (inductive) coupling between them. This interaction is analogous to the coupling observed in transformer windings, where the conductors are electrically and magnetically coupled. By tuning the parameters of such a model, the behavior of a transformer winding can be simulated. According to Fig. 4, there are various parameters to be optimized in this model. These parameters include the transmission line length, conductor spacing, shunt conductance, conductor radius, height of the conductors, ground resistance, and DC resistance. The initial values of these parameters are provided in Table I.

**Table 1.** Initial Values of the Model Parameters for the Conductors.

Parameter	Value
Radius	0.02 m
DC resistance	$50 \Omega/\text{km}$
Height	100 m
Spacing	Center
Shunt conductance	10 <sup>-7</sup> S/m

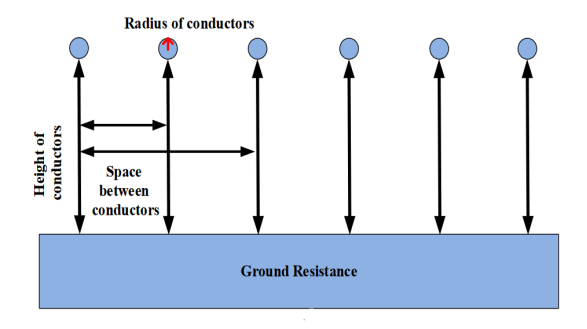


Fig 4. The geometric arrangement of the conductors in the simulation.

PSO optimizes these parameters by minimizing an objective function (OF) that measures the alignment between the simulated and experimentally measured transfer functions. This OF comprises two indices: the correlation coefficient (CC), representing the shape similarity between the vectors, and the Euclidean distance (ED), representing the vector distance. These indices are calculated as follows:

$$OF = (1 - CC)^2 + ED$$
 (18)

$$CC = \frac{\sum_{i=1}^{N} X(i)Y(i)}{\sqrt{\sum_{i=1}^{N} [X(i)]^{2} \sum_{i=1}^{N} [Y(i)]^{2}}}$$
(19)

$$ED = \|X - Y\| = \sqrt{\sum_{i=1}^{N} (Y(i) - X(i))^2}$$
 (20)

The OF used in this study quantifies the difference between the simulated and measured transfer functions of the transformer winding. Specifically, let *X* represent the simulated transfer function and *Y* the measured (experimental) transfer function; the OF is designed to minimize the discrepancy between these two vectors. This approach guides the PSO algorithm to iteratively adjust model parameters so that the simulation output closely matches the real winding behavior.

The basis for selecting this OF lies in its direct reflection of modeling accuracy. Since the goal is to reproduce the frequency response measured by FRA, minimizing the difference between the simulated and measured transfer functions provides a physically meaningful and computationally efficient target. Similar formulations have been adopted in previous works on transformer modeling and parameter identification, where accurate replication of resonance features and amplitude behavior across the frequency spectrum is critical. By using this objective function, the optimization process is tightly aligned with the practical goal of improving diagnostic fidelity.

PSO operates by initializing a swarm of particles, each representing a potential solution. The particles move within the search space based on their current position, their best-known position, and the best-known position found by any particle in the swarm. The velocity and position updates are governed by the following equations:

$$v_i^{k+1} = wv_i^k + c_1 r_1 (p_i^k - x_i^k) + c_2 r_2 (p_g^k - x_i^k)$$
(21)

$$x_i^{k+1} = x_i^k + v_i^{k+1} (22)$$

where  $v_i^k$  and  $x_i^k$  are the velocity and position of particle i at iteration k,  $p_i^k$  is the particle's best-known position,  $g^k$  is the global best position,  $c_1$  and  $c_2$  are acceleration constants,  $r_1$ , and  $r_2$  are random numbers between 0 and 1, and w is the inertia weight, which controls the balance between global and local exploration.

enhance the PSO algorithm's efficiency, appropriate lower and upper bounds for each parameter need to be set. This restriction confines the search to a specific range, improving the algorithm's speed and increasing the likelihood of identifying optimal parameters, especially in systems with multiple operational points. Effective bound management is the key feature of PSO. Particle positions are constrained within predefined lower and upper limits (lb and ub), ensuring parameters remain within feasible and physically meaningful ranges. This prevents invalid configurations that could disrupt the simulation. As the optimization progresses, the algorithm narrows these bounds dynamically around the best-found parameters, refining the search space and focusing computational efforts on the most promising regions. Based on trial and error, the shunt conductance of the conductors must not exceed  $10^{-6}$  S/m.

In this PSO implementation, the velocity update equation includes coefficients that balance the influence of each particle's individual experience with the collective knowledge of the swarm. These coefficients are multiplied by random factors, introducing a stochastic element that diversifies particle search paths and helps avoid local minima. Additionally, the velocities are scaled by a constriction factor (0.729) to stabilize particle movement, preventing divergence while preserving enough flexibility to explore the solution space. By integrating these enhancements, PSO significantly improves the accuracy and efficiency of parameter estimation in the MTL model, leading to better transformer behavior representation and more reliable diagnostic insights.

# 2.3 Integration of PSCAD and Python for Efficient Simulations

To facilitate real-time model tuning and simulation, PSCAD and Python are integrated using the **pywin32 library**. This integration allows Python to control PSCAD simulations, adjust model parameters automatically based on PSO outputs, and retrieve simulation results for evaluation. By leveraging Python's computational capabilities and PSCAD's transient simulation accuracy, this setup streamlines the optimization process, reducing manual intervention and improving efficiency.

The overall workflow of the modeling optimization process is illustrated in Fig. 5, which also highlights the key steps involved in the PSO algorithm. The process begins with Python initializing the optimization routine by randomly assigning initial values to the parameters of the MTL model, such as conductor spacing, self-inductance, and mutual coupling terms. These initial parameters are passed to PSCAD, which executes the first simulation to generate a baseline response. Subsequently, PSO initializes a population of candidate solutions (particles), each representing a possible set of MTL parameters. The OF, which quantifies the mismatch between simulated and experimental FRA reference, is evaluated for each particle. The algorithm then updates the personal best position of each particle and the global best among the swarm, guiding the search process. Particle velocities and positions are updated accordingly, and the newly generated parameter sets are passed again to PSCAD for simulation. The results are fed back to Python for reevaluation of the OF. This iterative loop—comprising simulation, evaluation, and parameter update—continues until a predefined stopping criterion is met (e.g., maximum number of iterations).

PSCAD's frequency-dependent phase-solving capabilities are particularly valuable for accurately modeling high-frequency behaviors, such as skin effects, eddy currents, and transient over-voltages. This ensures that transformer responses under different operating conditions are well-represented. By automating iterations and reducing computational overhead, the integration of PSCAD and Python enhances simulation accuracy, accelerates optimization, and improves transformer diagnostics. This combined approach provides a robust framework for high-frequency transient analysis and predictive maintenance.

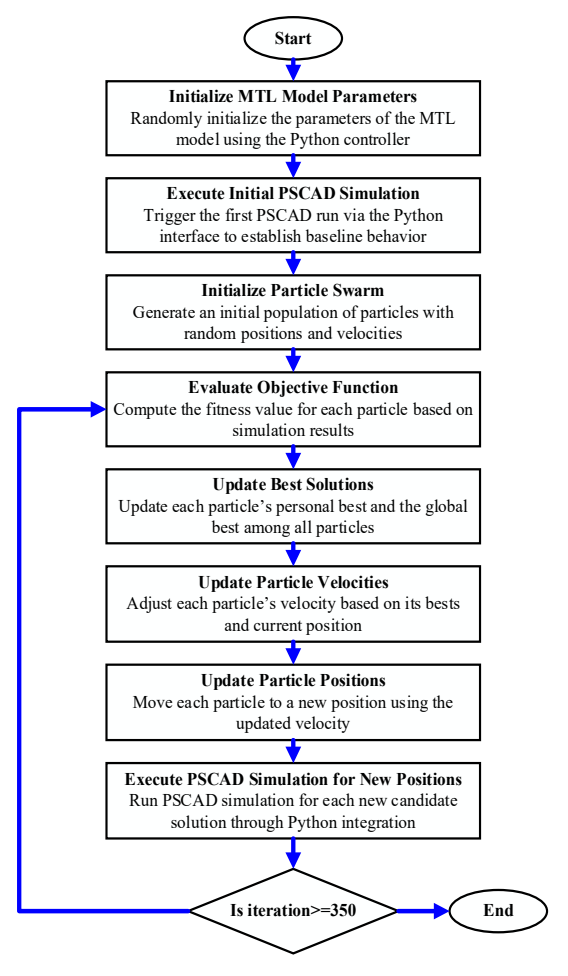


Fig 5. Workflow of the modeling process.

# 2.4 Validation against Experimental Transformer Data

The improved MTL model is validated using empirical data from a real transformer winding configured with a continuous disc high-voltage (HV) winding and a low-voltage (LV) helical winding. The HV winding consists of 60 discs, each containing 11 turns, while the LV winding comprises 24 turns, each turn formed by 12 parallel conductors. Fig. 6 illustrates the winding dimensions used in this study and the real winding in the laboratory as well.

To simulate the core and tank potentials of the transformer, two aluminum cylinders are incorporated into the test setup. Although actual power transformers typically use silicon steel for the core and steel for the tank, these materials primarily influence FRA results only up to a few kHz due to their magnetization characteristics. Beyond 10 kHz, the frequency response is dominated by the capacitances between the windings and adjacent plates, such as the core and tank, rendering the specific magnetic properties of the core material less significant.

Thus, aluminum cylinders are chosen as a practical substitute, ensuring that the test setup accurately represents the high-frequency response characteristics without the need for the exact core materials [3]. The frequency range below 10 kHz is not included in this evaluation, as the study focuses on high-frequency transient events. By replicating the transformer's core and tank potentials with aluminum cylinders, the setup effectively simulates the real transformer's electrical environment, providing reliable data for validating the MTL model's performance. These cylinders can be seen in Fig. 6(b).

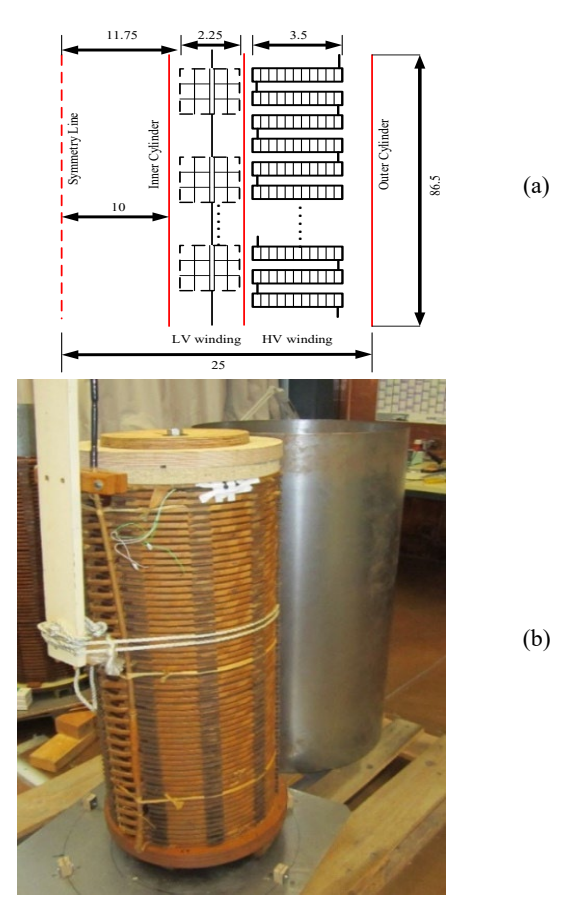


Fig 6.(a) The geometry of the case study transformer winding (dimensions in cm) and (b) its picture.

The transfer function of the MTL models is obtained in the simulation as the end-to-end open-circuit transfer function measured from the transformer as depicted in Fig. 7(a). This arrangement is one of the most common connection types in the FRA measurement method. The same circuit and procedure are exactly implemented in the software as shown in Fig. 7(b). Especially, the inclusion of  $50\Omega$  resistors, which are internally located in the FRA instrument, should be included in the simulation.

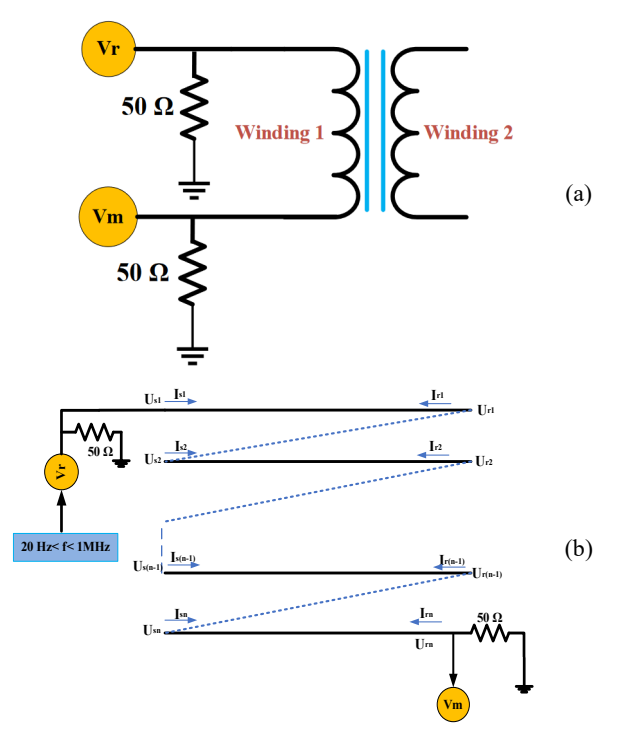


Fig 7.(a) End-to-end open-circuit measurement of the transfer function of a transformer winding, (b) implementation of this measurement configuration in the MTL model.

# 3 Results

This section presents the simulation results of the three MTL-based transformer models, each optimized using PSO and evaluated against experimental FRA measurements. In addition, a comprehensive sensitivity analysis is included to assess the physical influence of key parameters on the system's frequency response and to justify the necessity of optimization.

#### 3.1 Model response

#### The basic MTL model:

The results of the basic MTL model alongside the experimental data are shown in Fig. 8. As can be seen, the basic MTL model exhibits a similar decreasing trend to the real FRA measurements, indicating a reduction in amplitude at higher frequencies. Additionally, the model shows a correlation of over 93% with the real data, suggesting that it performs well and accurately captures

the system's overall behavior. However, the vertical discrepancy between the two curves may stem from the model's inability to fully account for damping effects. In real systems, series and parallel resistances contribute to greater signal attenuation at specific frequencies, while the model does not fully simulate these effects. To minimize this discrepancy and improve alignment with the real data, resistances should be incorporated, along with other model parameters, into the optimization process. This would help better simulate damping at higher frequencies and enhance the model's accuracy in replicating the characteristics of the real system. This is the main reason why the improved models are suggested in this study.

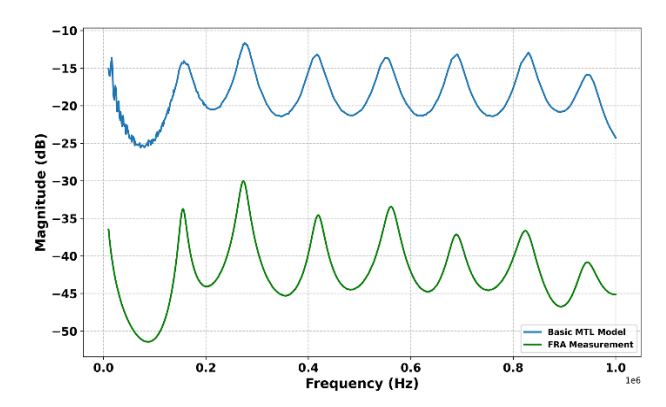


Fig 8.Comparison between the basic MTL model response and the FRA measurement.

#### **Improved MTL model 1:**

As shown in Fig. 9, the improved MTL 1 model significantly improves alignment with the real FRA measurements. The inclusion and optimization of series and ground-connected resistances in the model contributed to this improvement by capturing key damping effects and signal attenuation observed in the real system. The series resistances account for energy losses along the conductors, while the ground-connected resistances simulate dielectric and conductive losses to the ground. These optimized adjustments have enabled the model to better replicate the system's behavior, particularly at resonance points and in higher frequency ranges. Although some minor vertical discrepancies remain at specific frequencies, the overall alignment between the model and the real data has improved substantially. These results highlight the effectiveness of incorporating and optimizing resistive elements in the modeling process.

#### **Improved MTL model 2:**

As shown in Fig. 10, the improved MTL model 2 demonstrates improved alignment with the real FRA measurements compared to previous versions. This improvement is achieved by incorporating frequency-dependent dielectric resistive losses into the model.

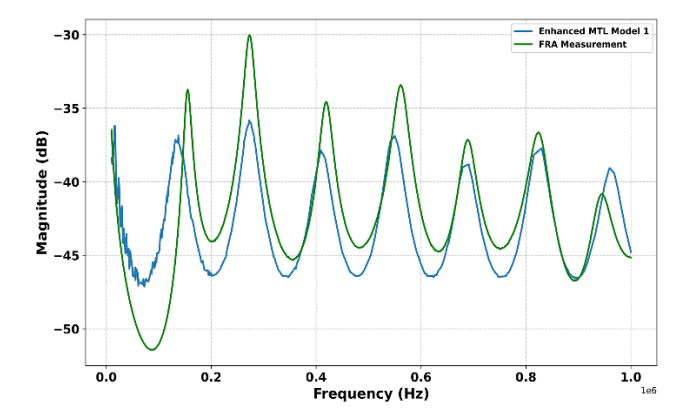


**Fig 9.**Comparison between the improved MTL 1 model response and the FRA measurement.

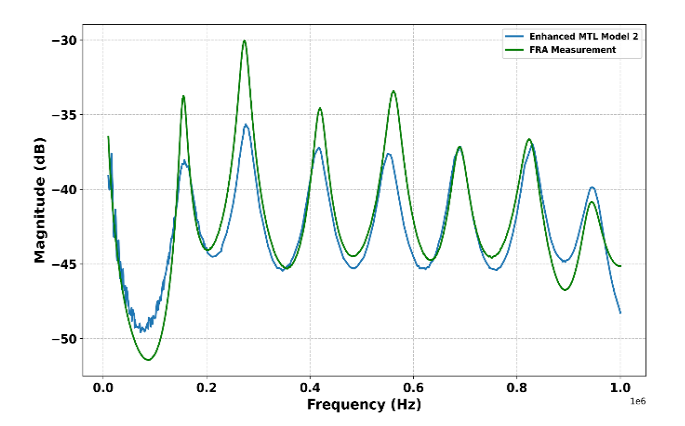


Fig 10.Comparison between the improved MTL 2 model response and the FRA measurement

These losses play a crucial role in accurately simulating the damping effects and signal attenuation observed in real systems, particularly at higher frequencies. By accounting for frequency-dependent dielectric resistive losses, the model captures the behavior of the dielectric and conductive elements more effectively. This adjustment allows the model to replicate the system's response more precisely across a wide frequency range, including both resonance points and higher frequency regions. The alignment between the model response and the FRA measurements shows significant improvement, with a reduced vertical discrepancy between the two curves.

These results underscore the importance of including frequency-dependent dielectric resistive losses in the modeling process. Such adjustments enhance the model's ability to simulate the real system's dynamic behavior and improve the overall fidelity of the frequency response analysis. To demonstrate the effectiveness of the proposed improvements, a quantitative comparison of the Basic MTL, Improved MTL 1, and Improved MTL 2 models is carried out. Table II presents the *ED*, *CC*, and the overall OF value

for each model. These metrics highlight the enhanced accuracy achieved through each modeling refinement.

**Table 2.** Quantitative comparison of simulation accuracy.

Model	Euclidean	Correlation	Objective
	Distance	Coefficient	Function
Basic MTL	716.5	0.932	717.468
Improved MTL 1	55.24	0.832	55.932
Improved MTL 2	51.88	0.939	51.761

#### 3.2 Sensitivity Analysis of Model Parameters

To evaluate the influence of model parameters on the transformer's frequency response, a parametric study was conducted. In each case, one parameter was varied while the others remained fixed, and the resulting impact on the transfer function was analyzed. This study demonstrates the physical significance of each parameter and supports the necessity of parameter tuning through optimization.

## **Transmission Line Length:**

Figure 11 shows the frequency response for transmission lines of 0.1 km, 0.2 km, and 0.3 km. The simulation results indicate that, with increasing line length, both the resonance and anti-resonance frequencies shift to lower values, while no significant change in magnitude is observed. This demonstrates that line length significantly influences the position of resonant peaks, although the overall amplitude remains largely unaffected.

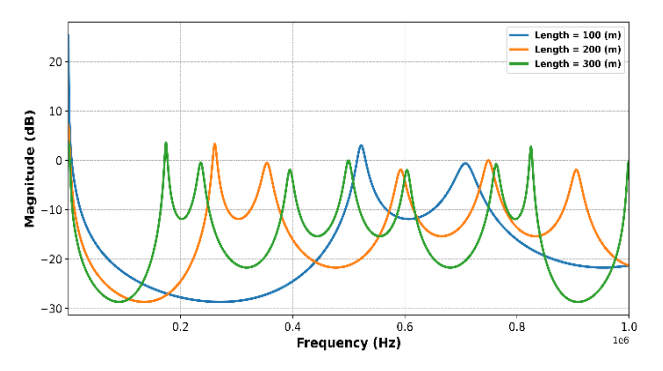


Fig 11.Effect of Transmission Line Length on the Frequency Response

### **Horizontal Spacing Between Conductors:**

Figure 12 illustrates that increasing the conductor spacing shifts the resonances and anti-resonances up to a specific frequency value. Beyond this point, the trend reverses, indicating a nonlinear relationship between spacing and frequency response. This variation, however, has only a minor influence on the magnitude.

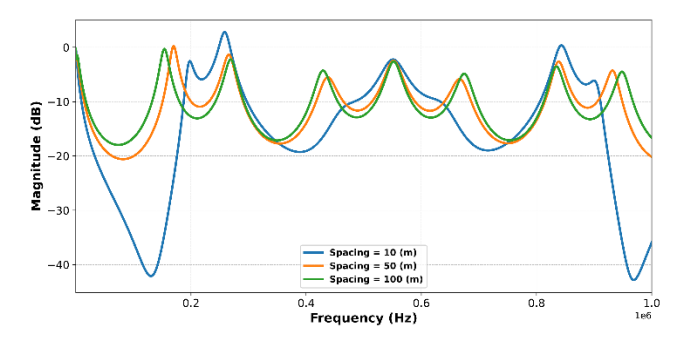


Fig 12.Effect of Horizontal Spacing Between Conductors on the Frequency Response

# **Height of Conductors Above Ground:**

Figure 13 shows the effect of conductor height (15 m, 25 m, 40 m) on frequency response. Greater height reduces capacitive coupling to ground, increasing high-frequency magnitude. Resonance peaks shift slightly to lower frequencies, and the response becomes smoother and more damped.

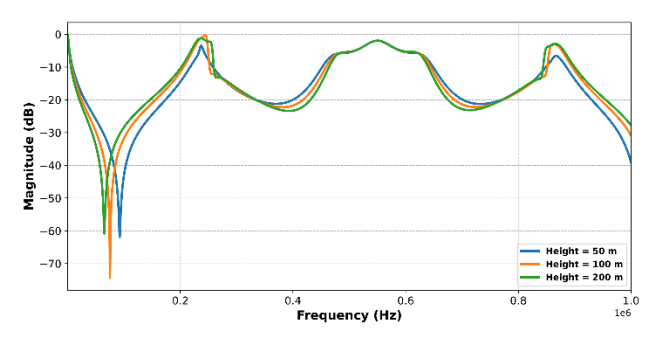


Fig 13.Effect of Height of the Conductors on the Frequency
Response

#### **Conductor Radius:**

Figure 14 presents the effect of conductor radius (0.02 m, 0.05 m, 0.07 m) on frequency response. Smaller radii slightly shift resonances to higher frequencies with sharper peaks, while larger radii cause broader peaks at lower frequencies. The impact is noticeable but not substantial.

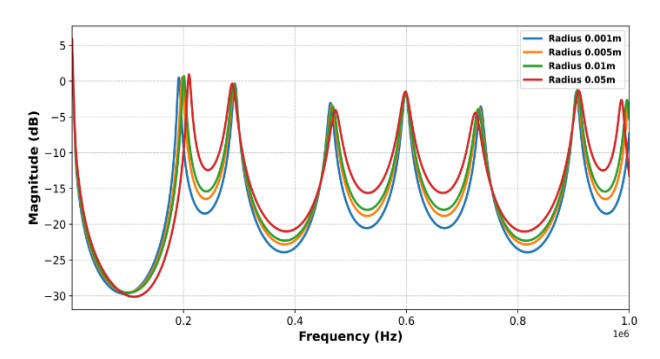


Fig 14.Effect of the Height of the Radius of the Conductors on the Frequency Response

#### - DC Resistance of Conductors:

Figure 15 compares the responses for DC resistance values of 5  $\Omega$ , 30  $\Omega$ , and 50  $\Omega$ . Increased DC resistance dampens the resonance peaks without noticeably shifting their frequency positions. For example, the 50  $\Omega$  case shows substantial peak attenuation compared to the 5  $\Omega$  case. This indicates that while resistance affects the amplitude and damping of the response, it does not alter the resonance frequencies themselves.

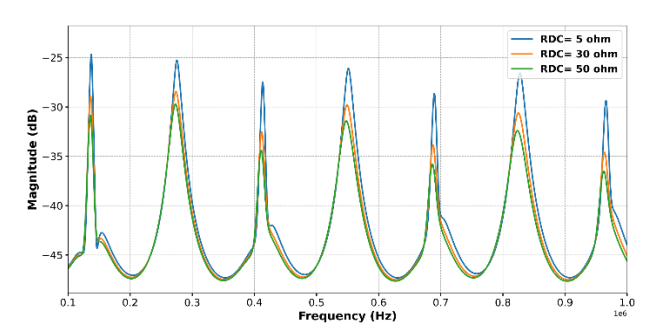


Fig 15.Effect of Height of the DC Resistance of the Conductors on the Frequency Response

#### **Shunt Conductance:**

Figure 16 studies the effect of shunt conductance on the frequency response. Four values (1e<sup>-6</sup>, , 5e<sup>-7</sup>, 1e<sup>-8</sup>, and 1e<sup>-12</sup> S/m) are compared. Noticeable drops in amplitude are observed with increasing conductance, but the resonance frequencies do not change, with only the amplitude increasing at lower values until it eventually stabilizes.

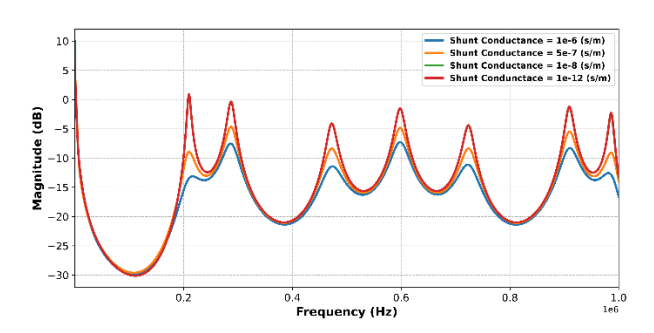


Fig 16.Effect of the Shunt Conductance on the Frequency
Response

#### **Ground Resistivity:**

Figure 17 investigates the impact of ground resistivity values:  $0.1 \ \Omega.m$ ,  $50 \ \Omega.m$ , and  $150 \ \Omega.m$ . Lower ground resistivity  $(0.1 \ \Omega.m)$  causes broader, more damped peaks, whereas higher resistivity  $(150 \ \Omega.m)$  yields sharper, higher-amplitude peaks. Despite these differences in amplitude, the positions of the resonance frequencies are largely unaffected. This suggests that ground resistivity primarily governs damping rather than resonance location.

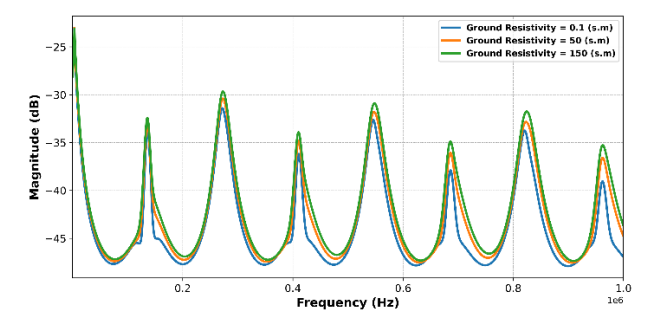


Fig 17.Effect of Ground Resistivity on the Frequency Response

It is important to highlight the real-world applicability of this modeling approach by defining the scenario. Initially, the intact FRA data of a transformer is input into the algorithm, establishing a baseline model. The investigation presented in this paper focuses solely on this initial step. In the event of a fault suspicion, a newly measured FRA, indicative of the transformer's potentially faulty condition, is fed back into the algorithm. A new model is then generated, which is subsequently compared to the baseline model. This comparison reveals the changes in the parameters of the transmission line model from the intact to the faulty state. By analyzing these changes, the fault within the transformer can be identified. For instance, an increase in the capacitive coupling between a winding and the earth in the faulty condition suggests that the winding may have shifted toward a grounded area, such as a buckle in the low-voltage windings. The identification of fault types based on these parameter changes remains a direction for future work in this study.

#### 4 Conclusion

This study presents an advanced MTL modeling approach to address the challenges in transformer highfrequency transient and frequency response analysis. improved models incorporate The significant innovations, including the optimization of parameters through PSO, the inclusion of both series and groundconnected resistances, and the modeling of frequencydependent dielectric resistive losses. The results demonstrate the effectiveness of these enhancements in accurately capturing high-frequency behaviors and reducing discrepancies between simulated and measured FRA data. The first improved model significantly enhanced alignment by incorporating resistive losses, while the second model further refined accuracy by including frequency-dependent dielectric losses. These advancements allow for precise simulation of damping effects and better replication of real-world transformer responses, particularly at resonance points and in higher frequency ranges. By integrating PSCAD and Python, this study also streamlines the simulation process, reducing computational overhead while maintaining high fidelity. The proposed models provide a robust foundation for applications in transformer diagnostics, predictive maintenance, and design optimization, contributing to the reliability and resilience of modern power systems. Future work may explore additional loss mechanisms and refine the models for broader transformer designs and operational conditions.

#### **Conflict of Interest**

The authors declare no conflict of interest.

#### **Author Contributions**

A.E.: Methodology, Software, Validation, Writing – Original Draft, Visualization

M.H.S.: Conceptualization, Methodology, Formal Analysis, Writing – Review & Editing, Project Administration

A.A.S.A.: Supervision

#### References

- [1] A. Esmaeilvandi, M. H. Samimi, and A. A. Shayegani Akmal, "High-Frequency Traveling Wave Modeling of Transformers for Frequency Response Analysis," The 4th International Conference on Electrical Machines and Drives (ICEMD 2024), Tehran, Iran, Dec. 10–11, 2024.
- [2] F. Nasirpour, A. Heidary, M. G. Niasar, A. Lekić, and M. Popov, "High-frequency transformer winding model with adequate protection," Electric Power Systems Research, vol. 223, p. 109637, Jun. 2023.
- [3] M. F. M. Yousof, C. Ekanayake, and T. K. Saha, "Frequency response analysis to investigate deformation of transformer winding," IEEE Transactions on Dielectrics and Electrical Insulation, vol. 22, no. 4, pp. 2359–2367, Aug. 2015.
- [4] M. H. Samimi, S. Tenbohlen, Amir, and H. Mohseni, "Effect of Different Connection Schemes, Terminating Resistors and Measurement Impedances on the Sensitivity of the FRA Method," IEEE Transactions on Power Delivery, vol. 32, no. 4, pp. 1713–1720, May 2016.
- [5] Y. Alkraimeen and P. Gomez, "On the Computation of Frequency-Dependent Core and Proximity Effects for Transient Analysis of Transformer Windings," IEEE Transactions on Power Delivery, vol. 34, no. 3, pp. 891–898, Feb. 2019.
- [6] M. Popov, R. P. P. Smeets, and J. L. Roldan, "Analysis of Very Fast Transients in Layer-Type Transformer Windings," IEEE Transactions on Power Delivery, vol. 22, no. 1, pp. 238–247, Jan. 2007.

- [7] Z. Luna Lopez, P. Gomez, F. P. Espino-Cortes, and R. Pena-Rivero, "Modeling of Transformer Windings for Fast Transient Studies: Experimental Validation and Performance Comparison," IEEE Transactions on Power Delivery, vol. 32, no. 4, pp. 1852–1860, Aug. 2017.
- [8] S. M. H. Hosseini, M. Vakilian, and G. B. Gharehpetian, "An Improved MTL Modeling of Transformer Winding," 7th International Conference on Power Systems Transients, Lyon, France, Jun. 4–7, 2007.
- [9] G. Liang, S. Gao, Y. Wang, Y. Zang, and X. Liu, "Fractional transmission line model of oil-immersed transformer windings considering the frequencydependent parameters," IET Generation, Transmission & Distribution, vol. 11, no. 5, pp. 1154–1161, Mar. 2017.
- [10] T. Y. Ji, W. H. Tang, and Q. H. Wu, "Detection of power transformer winding deformation and variation of measurement connections using a hybrid winding model," Electric Power Systems Research, vol. 87, pp. 39–46, Jun. 2012.
- [11] A. Shintemirov, W. H. Tang, and Q. H. Wu, "A Hybrid Winding Model of Disc-Type Power Transformers for Frequency Response Analysis," IEEE Transactions on Power Delivery, vol. 24, no. 2, pp. 730–739, Apr. 2009.
- [12] M. Gunawardana, F. Fattal, and B. Kordi, "Very Fast Transient Analysis of Transformer Winding Using Axial Multiconductor Transmission Line Theory and Finite Element Method," IEEE Transactions on Power Delivery, vol. 34, no. 5, pp. 1948–1956, Aug. 2019.
- [13] M. A. Sobouti, D. Azizian, M. Bigdeli, and G. B. Gharehpetian, "Multi-conductor Transmission Line Model of Split-winding Transformer for Frequency Response and Disk-to-disk Fault Analysis," International Journal of Engineering, Transactions C: Aspects, vol. 34, no. 6, 2021.
- [14] K. G. N. B. Abeywickrama, Y. V. Serdyuk, and S. M. Gubanski, "Exploring possibilities for characterization of power transformer insulation by frequency response analysis (FRA)," IEEE Transactions on Power Delivery, vol. 21, no. 3, pp. 1375–1382, Jul. 2006.
- [15]B. Gustavsen, "Frequency-dependent modeling of power transformers with ungrounded windings," IEEE Transactions on Power Delivery, vol. 19, no. 3, pp. 1328–1334, Jul. 2004.
- [16] H. Gong, J. Liu, Z. Jiang, J. Zhou, X. Fan, and D. He, "A Time-Domain Fractional Element Model for Aging Condition Analysis of Hot-Spot Region

- Insulation in Power Transformer," IEEE Transactions on Instrumentation and Measurement, vol. 73, pp. 1–11, 2024.
- [17] Q. Ding, Y. Yu, C. Xiong, and Z. D. Wang, "A modified lumped parameter model of distribution transformer winding," Global Energy Interconnection, vol. 3, no. 2, pp. 158–165, Jun. 2020.
- [18] Y. Yu, W. Zanji, C. Xiong, and Z. D. Wang, "Improved lumped parameter model for transformer fast transient simulations," IET Electric Power Applications, vol. 5, no. 6, pp. 479–479, Jan. 2011.
- [19] Z. Azzouz, A. Foggia, L. Pierrat, and G. Meunier, "3D finite element computation of the high-frequency parameters of power transformer windings," IEEE Transactions on Magnetics, vol. 29, no. 2, pp. 1407–1410, Mar. 1993.
- [20] N. Abeywickrama, Y. V. Serdyuk, and S. M. Gubanski, "High-Frequency Modeling of Power Transformers for Use in Frequency Response Analysis (FRA)," IEEE Transactions on Power Delivery, vol. 23, no. 4, pp. 2042–2049, Oct. 2008.
- [21] E. Bjerkan and H. K. Høidalen, "High-frequency FEM-based power transformer modeling: Investigation of internal stresses due to network-initiated overvoltages," Electric Power Systems Research, vol. 77, no. 11, pp. 1483–1489, Sep. 2007.
- [22] M. Žarković and Z. Stojković, "Analysis of artificial intelligence expert systems for power transformer condition monitoring and diagnostics," Electric Power Systems Research, vol. 149, pp. 125–136, Aug. 2017.
- [23] E. Rahimpour, V. Rashtchi, and H. Shahrouzi, "Applying artificial optimization methods for transformer model reduction of lumped parameter models," Electric Power Systems Research, vol. 84, no. 1, pp. 100–108, Mar. 2012.
- [24] J. W. Nims, R. E. Smith, and A. A. El-Keib, "Application of a Genetic Algorithm to Power Transformer Design," Electric Machines & Power Systems, vol. 24, no. 6, pp. 669–680, Sep. 1996.

# **Biographies**



Ali Esmaeilvandi was born and raised in Eizeh, Iran. He received a Bachelor's degree in Electrical Engineering from Isfahan University of Technology in 2022 and is currently pursuing a degree Master's in Power Systems at the University of Tehran. His thesis focuses on high-frequency transformer

modeling using traveling wave theory for Frequency Response Analysis (FRA). He has hands-on experience in high-voltage laboratories, including partial discharge testing and insulation diagnostics, and has served as a Teaching Assistant and as a member of the Execution Team at the 19th International Conference on Protection & Automation in Power Systems. His research interests include high-voltage technology, artificial intelligence in power systems, and fault detection.



Mohammad Hamed Samimi received his Ph.D. in Electrical Engineering from the University of Tehran, Iran, in 2017. During his doctoral studies, he conducted part of his research at the University of Stuttgart, Germany, through the DAAD scholarship award for the "bi-nationally supervised doctoral degree" program in 2015 and 2016.

He has worked as a Researcher at the Power System Protection Office of the Iran Grid Management Company for two years. Currently, he is an Associate Professor of Electrical Engineering at the School of Electrical and Computer Engineering, University of Tehran. His research interests focus on the modeling, condition monitoring, and diagnosis of high-voltage apparatuses. Dr. Samimi has been recognized for his outstanding contributions to education, receiving the "Excellence in Teaching Award" from the University of Tehran in 2023 and the national "Sheikh Mofid" award for Finest Educating Professors from Iran's National Elites Foundation.